

13th CIRP Conference on Photonic Technologies [LANE 2024], 15-19 September 2024, Fürth, Germany

## Evaluation of different surface topography measurement methodologies for characterizing weld beads in shipbuilding

Li-Wei Hsu<sup>a\*</sup>, Saeid Parchegani Chozaki<sup>a</sup>, Kandice Suane Barros Ribeiro<sup>a</sup>, Wallace Moreira Bessa<sup>a</sup>, Antti Salminen<sup>a</sup>

<sup>a</sup>Department of Mechanical and Materials Engineering, University of Turku, Joukahaisenkatu 3-5 B, Turku 20520, Finland

\* Corresponding author. E-mail address: [li-wei.hsu@utu.fi](mailto:li-wei.hsu@utu.fi)

### Abstract

The weld bead is crucial in identifying defects during laser welding, aiding in the evaluation of weld strength and quality. However, accurately monitoring and identifying defects with cameras can be challenging in the preassembly phase. This paper compares surface topography of laser weld beads using in-process Optical Coherence Tomography (OCT) and post-process Focus Variation Microscopy (FVM). Both techniques were employed on welded A36 structural steel plates to detect the surface defects. The weld profile was evaluated according to EN ISO 13919-1, and the quality level B was given to the surface topography measurement from both techniques. The correspondence between these two methodologies is imperative for implementing profile data in advanced monitoring systems. Thus, by reducing the delay between defect formation and inspection, this paper supports a more intelligent welding process, particularly in the shipbuilding industry.

© 2024 The Authors. Published by Elsevier B.V.

This is an open access article under the CC BY-NC-ND license (<https://creativecommons.org/licenses/by-nc-nd/4.0>)

Peer-review under responsibility of the international review committee of the 13th CIRP Conference on Photonic Technologies [LANE 2024]

*Keywords:* laser welding; bead geometry; inspection; optical coherence tomography; focus variation microscope, metrology

### 1. Introduction

Laser welding is a versatile joining method with high precision and flexibility applied in various industries, and the working dimension covers a few millimeters thick to several meters long. Its advantages include deep welds and high welding speed, as the keyhole, sometimes called vapor capillary, acts as a specific absorption area to convert the electromagnetic energy to thermal energy on the joint of metal workpieces. However, complex and dynamic physical phenomena are involved, such as recoil pressure, metal surface tension, heat transfer, laser beam absorptivity, that make it intricate to control the consistent quality. Common defects can form on the surface of a weld, like excess weld metal, incompletely filled groove, and undercut, while some defects take place inside a weld, such as closed pores and inclusions.

This research paper presents a method to evaluate the top surface quality of the weld by an algorithm which uses

percentage filter and regression analysis on the data from two types of surface topography measurement techniques, in-process optical coherence tomography (OCT) and post-process focus variation microscopy (FVM). Both techniques are based on optical imaging but by different principles, as the former one is on interference fringe pattern from low-coherence interferometry, while the latter one is on variation of relative distance to capture images at different focal planes.

OCT is an interferometric measuring method that enables the measurement of optical path distance based on the interference fringe pattern, and it has the advantage of imaging the subsurface structure with high acquisition rate, but the reflection may be affected by fumes, spatters, and dust [1,3]. FVM has higher lateral resolution which can be even enhanced by higher magnification objectives, but acquisition time can be much longer [2,4]. However, both optical techniques are susceptible to specular reflection, causing missing values in point clouds, as parallel light is reflected in the same direction.

## Nomenclature

FVM focus variation microscopy  
OCT optical coherence tomography

The proposed algorithm is capable of removing these values and exhibiting the pattern for data visualization and analysis. In addition, it can perform the coordinate transformation to eliminate the artifacts from the back side of the excessive penetration root that may induce the tilted plane and the intrinsic inclination of sample holders. Fig. 1. shows the illustrations and images of these two measurement techniques.

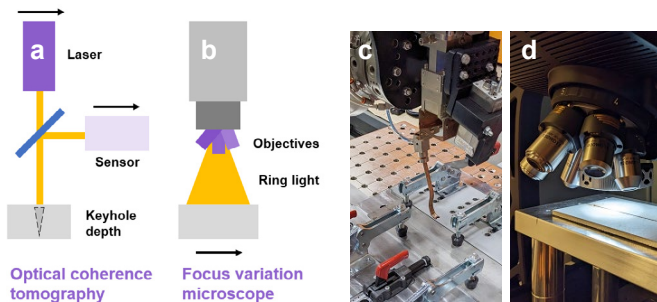


Fig. 1. (a) Illustration of optical coherence tomography; (b) Illustration of focus variation microscopy; (c) OCT setup image; (d) FVM setup image.

## 2. Methods

The laser welding experiment was conducted with in-process OCT monitoring and post-process FVM inspection on A36 steel plates of geometry 400x50x5 mm in the configuration of butt joint. When samples were cut with a laser, there were two alignment marks on the edge with 20 mm from both ends. Samples were clamped with the fixture to ensure there was no gap between the samples. The welding speed was 3 m/min, laser power 5.5 and 5 kW by an IPG fiber laser, the fiber core diameter was 300  $\mu\text{m}$ , collimation lens 150 mm and focusing lens focal length 348 mm, and no edge preparation was conducted on the edge of samples. The incidence angle of the laser beam was perpendicular to the surface plane of the steel plates, and the laser beam started in front of the first alignment and ended after passing the second alignment mark.

Light source of OCT was an infrared, continuous wave with wavelength in the 800 nm – 900 nm range, and the optical power was less than 20 mW. The measurement radiation was not affected by the process ration as the coherence condition was insufficient. Transverse profile distance was 8 mm lagging behind the keyhole area, and the scanning line was 4 mm long with 4  $\mu\text{m}$  intervals within.

The FVM was measured with InfiniteFocus by Bruker alicon, and its objective 1900 WD30 had working distance 30mm, lateral measurement range 3.8 mm, measurement point distance 1.77  $\mu\text{m}$ , measurement noise 80 nm, vertical resolution 250 nm. The sampling distance was 3.546  $\mu\text{m}$  with coaxial light, ring light and polarizer, and the vertical scanning microscope stitched the point cloud to form a combined image of 200 mm x 38 mm area.

The exported point cloud data was processed with MATLAB to analyze the matrix, and the flowchart in Fig. 2 showed the procedures for data processing and quantitative analysis. Data from both techniques went through some common steps, like data cleansing, three-dimensional visualization, weld profile two-dimensional plot, and baseline regression for defects evaluation, but FVM had more steps on coordination transformation based on the inclination tendency of the data. Meanwhile, statistical filtering like percentile filter was included to exclude the outlier values that were not correctly captured by the sensor.

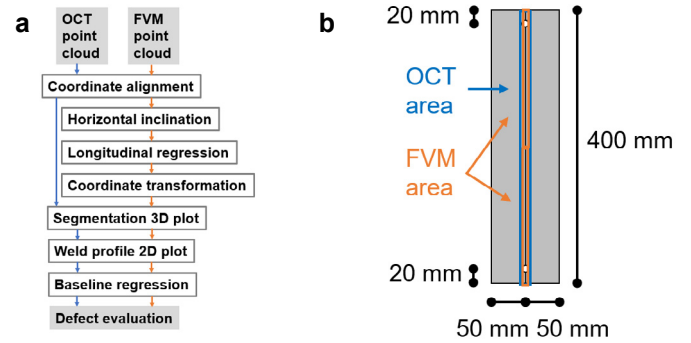


Fig. 2. (a) Algorithm flowchart on MATLAB; (b) The geometry of the workpiece and the scanning area by two techniques.

The percentile filter was set to only include the values within the range of 1 to 99 %, and it could be modified if excessive false reflection was present. The coordinate transformation was based on the linear regression along both longitudinal and transverse directions. For the regression of baseline of weld profile, the first quarter and the last quarter of the point cloud were selected to represent the surface of the workpiece, and the calculation of the defects was with Cartesian coordinates shown on Eq. 1

$$D = \frac{H}{\sqrt{1 + a^2}} \quad (1)$$

$D$  is the depth [ $\mu\text{m}$ ] of an incompletely filled groove,  $H$  is the difference of the vertical height [ $\mu\text{m}$ ] from data points, and  $a$  is the vector obtained from the regression without unit. To calculate the height of excess weld metal, it can be done by the subtraction of the other highest value above the baseline. The qualification of weld beads was done according to EN ISO 13919-1:2019 [5] which defines the maximum flaw dimensions to various flaw types in laser beam welding.

## 3. Results and discussion

As two laser powers were tested in this setup, the result from 5.5 kW is discussed first due to the fact that the penetration is full, and it has better mechanical properties. Instead, the sample with 5 kW shows lack of penetration. The surface topography is exported as point clouds, shown in Fig. 3, before being processed any designed algorithms.

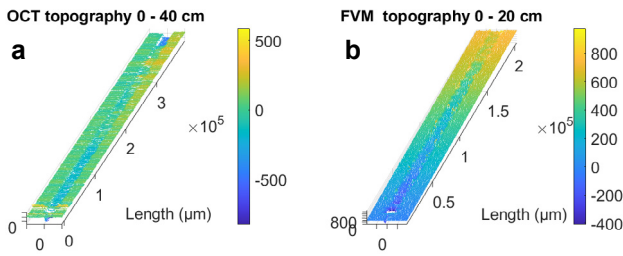


Fig. 3. The point cloud showing a horizontal plane from (a) OCT, but an inclination from (b) FVM based on the color gradient.

The result, shown in Fig. 3b from FVM, is tilted due to the intrinsic inclination of the substrate or the uneven bottom of the welded workpiece. Therefore, it is necessary to perform linear regression for coordinate transformations on FVM point cloud, but the situation is less notable for OCT point cloud with even longer length, 400 mm, compared to 200 mm of FVM.

Before the transformation, the alignment of the starting point can be done with a simple technique that counts the missing points around the region of alignment marks. For example, Fig. 4 shows that the second half of FVM point cloud has the vacancy located around 190 mm area, but the second alignment mark on the sample is located at 380 mm in reality. The compensation of the difference can be made numerically to align the sample for comparison on weld bead profile.

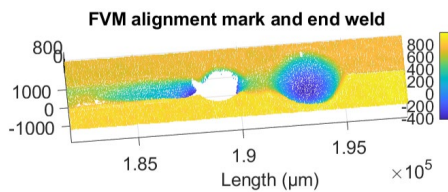


Fig. 4. Alignment mark and end weld measured with FVM.

To correct the horizontal level, the points are plotted in the transverse and longitudinal directions to illustrate the distribution. At the beginning part of the points are missing due to the predefined marks at 20 mm from the edge. Compared to transverse direction, the longitudinal direction has more significant inclination, meaning a deviation around 0.8 mm can occur at the end of the 200 mm long samples, shown in Fig. 5a, and a regression algorithm is used to bring the points to the horizontal plane according to its angle, the result is shown in Fig. 5b with homogeneous color throughout the sample.

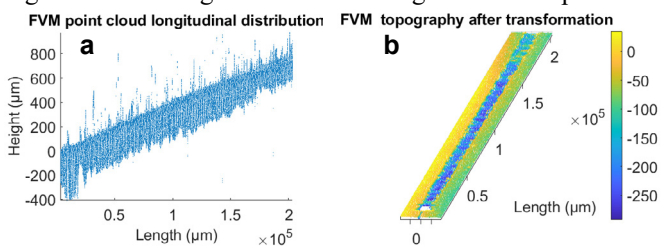


Fig. 5. (a) FVM point cloud height distribution along the longitudinal direction; (b) FVM topography after coordinate transformation.

To visually compare the results, the point cloud from the same segment, for example from 100 to 200 mm, is chosen for 3D scatter plot, and the same range on the same sample shows similar degree of extra weld metal and incomplete filled groove

in Fig 6. While the evaluation shows the same results, it is noted that lateral resolution from OCT point cloud is much lower than FVM data, and sparse point cloud may miss the detailed surface structure that contains defects for crack initiation.

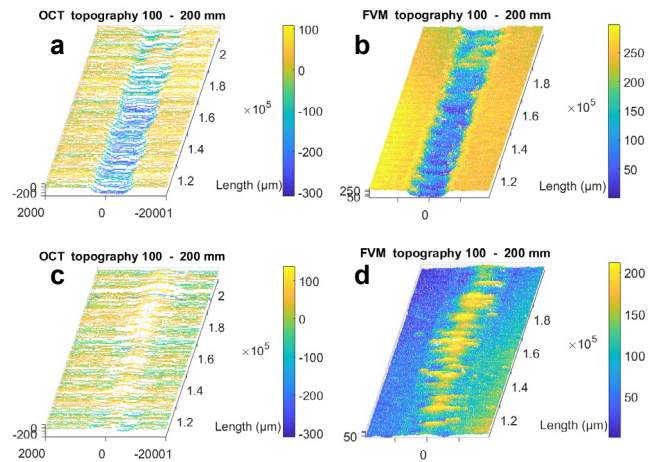


Fig. 6. Topography of the region from 100 to 200 mm of 5.5 kW laser with (a) OCT and (b) FVM methods, and 5 kW with (c) OCT and (d) FVM.

Then the same algorithm is used on the sample laser welded with 5 kW power, whose surface shows excess weld metal in the selected region, shown in Fig 6. For FVM topography, the result is promising, and little specular reflection can be seen from a few missing points. However, OCT results contain many artifacts, which stem from the false reflection and are removed by percentile filters to lose more points than the former parameter that results in full penetration.

In addition to segmentation 3D plots, weld profile 2D plots can be further examined at specific sections to compare the two techniques. Based on EN ISO 13919-1:2019 standard, 5 mm samples used in this research paper can be evaluated with quality level B when excess weld metal is less than 950  $\mu\text{m}$  and the incompletely filled groove is less than 500  $\mu\text{m}$  [5]. Without considering other criteria, such as excessive penetration or root overlap, the profile of the top surface obtains the highest quality level at the chosen sections in Fig 7. Note that the difference of resolution can be seen from the sparse point cloud in Fig 7a. The weld profile is coherent, and the measurements of defects are around 10% deviations.

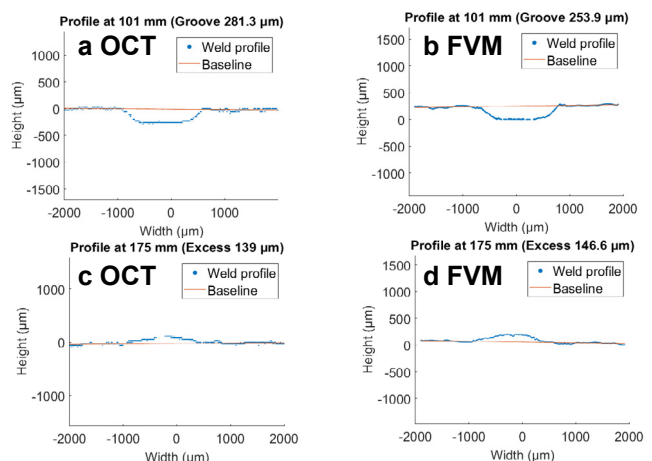


Fig. 7. Weld bead profile at the 101 mm of 5.5 kW with (a) OCT and (b) FVM, and at 175 mm of 5.0 kW with (c) OCT and (d) FVM.

For the set with lower laser power 5 kW, the groove is not observed, and excess weld metal is more prevalent. The result corresponds with the fact that the weld has a lack of penetration and that the melt did not manage to flow through the other side of the sample. The calculation of excess weld metal is deviated, and it is due to that the baseline of OCT point cloud was not well calculated with the regression on the first and last quarter of point cloud profile with low vertical resolution.

The minor difference of surface topography measured by OCT and FVM can be attributed to instruments or the difference of volume of weld after complete solidification. As the lagging distance of OCT is set at 8 mm, which is around the boundary of the melt pool, the scanning area of the transverse profile may be on the melt pool or the incomplete solidified weld. Despite these issues, the correspondence of the best results shows the positive correlation. The thorough examination is carried out and shown in Fig 8. Both techniques present the corresponding results that both extra weld metal and incompletely filled groove fit into the category of class B. Comparing OCT results on two laser power inputs, the groove depth is more significant for the 5.5 kW set, and the tendency can be observed on the FVM results too. Another finding is that the second half of the 5.5 kW results tend to diverge more than the lower power set, but the shallower groove is a good sign for better quality until it approaches the alignment mark.

About the in-house developed algorithms, the parameters for these percentile filters can be individually adjusted based on each weld bead profile, and it can be potentially trained to recognize the pattern after collecting sufficient data for classification tasks with a machine learning algorithm.

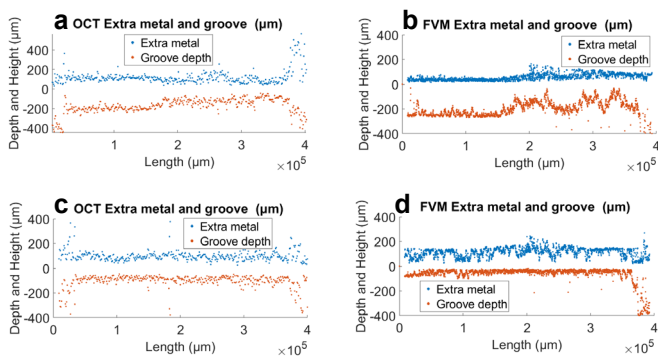


Fig. 8. Weld bead profile evaluation of the two samples in full length 5.5 kW with (a) OCT and (b) FVM, and 5 kW with (c) OCT and (d) FVM.

Table 1. Comparison of the two techniques on 400 mm samples

Method	OCT	FVM
Stage	In-process	Post-process
Moving	Sensor	Sample
Acquisition time	Less than 10 seconds	More than 10 minutes
Point cloud file size	Less than 10 MB	More than 1000 MB
Keyhole measurement	Able	Unable
Lateral resolution	4x1000 μm	7x7 μm
Vertical resolution	20 μm	0.25 μm
Scanning density	250 points/mm <sup>2</sup>	19000 points/mm <sup>2</sup>

The potential of the digitalized surface topography data is that the area between the profile and the baseline can be calculated, instead of merely measuring the distance as the current standard suggests. From the perspective of the algorithm, the area can provide a more robust evaluation as one single false reflection is not able to mislead the judgment.

To summarize, Table 1. shows the comparison of these two techniques and points out the feasibility when it is applied in the academic and industrial cases of efficiency and precision for higher automation in manufacturing. OCT can be applied in-process during the laser welding in an instant manner with fast signal processing methods, while the vulnerability to the fumes and spatter close to the melt pool may deliver unreliable results. FVM is more precise, but the longer acquisition time and larger production lines with a significant amount of data.

#### 4. Conclusion

The paper presents the results of the two optical imaging techniques for surface weld bead shape based on two distinct principles, and the algorithms developed for these two instruments can be applied in any future experiments to quantitatively evaluate weld quality. OCT, as a common technique to measure keyhole depths, can be used to measure the transverse profile then form the surface topography, showing that the results are coherent to FVM. The successful implementation with regression model and percentile filter in laser welding monitoring is a solid foundation for the future digitalization of manufacturing. Regression and classification problems can be solved with higher autonomous levels by training of machine learning algorithms with more laser welding experiments.

#### Acknowledgements

The research team acknowledges for the project CaNeLis - Carbon-neutral lightweight ship structures using advanced design, production, and life-cycle services, funded by Business Finland (3360/31/2022) Meyer Turku Oy, Cavitar Oy and SSAB Oyj. Project is part of NEcOLEAP leading company of Meyer Turku Oy.

#### References

- [1] Boley, M., Fetzer, F., Weber, R., & Graf, T. (2019). Statistical evaluation method to determine the laser welding depth by optical coherence tomography. *Optics and Lasers in Engineering*.
- [2] Gao, W., Haitjema, H.H., Fang, F., Leach, R.K., Cheung, C.F., Savio, E., & Linares, J. (2019). On-machine and in-process surface metrology for precision manufacturing. *CIRP Annals*.
- [3] Werner, M.K., Wagner, J., Ribbeck, F., Hensel, S., Goth, K., Graf, T., & Meschut, G. (2022). Influence of the incident angle on the OCT measurement during remote laser beam welding. *Procedia CIRP*.
- [4] Syam, W.P., Rybalcenko, K., Gaio, A., Crabtree, J., & Leach, R.K. (2019). Methodology for the development of in-line optical surface measuring instruments with a case study for additive surface finishing. *Optics and Lasers in Engineering*.
- [5] International Organization for Standardization. (2019). Electron and laser-beam welded joints. Requirements and recommendations on quality levels for imperfections. <https://www.iso.org/standard/75514.html>